Available online at www.sciencedirect.com
ScienceDirect
Journal of Organometallic Chemistry 692 (2007) 5621–5632
Journal of Organometallic Chemistry
www.elsevier.com/locate/jorganchem

Synthesis, IR-, NMR-, DFT and X-ray study of ferrocenyl heterocycles from thiosemicarbazones. Part 21: Study on ferrocenes

Balázs Fábián [a], Veronika Kudar [a], Antal Csámpai [b,*], Tibor Zs. Nagy [a], Pál Sohár [a,b,*]

[a] *Research Group for Protein Modelling, Hungarian Academy of Sciences, Eötvös Loránd University, P.O. Box 32, H-1518 Budapest 112, Hungary*
[b] *Institute of Chemistry, Eötvös Loránd University, P.O. Box 32, H-1518 Budapest 112, Hungary*

Received 22 March 2007; received in revised form 22 August 2007; accepted 24 September 2007
Available online 29 September 2007

Abstract

Cyclization reactions of the thiosemicarbazones of formyl- and acetylferrocene and their *S*-methyl derivatives with DMAD afforded novel ferrocenyl-hydrazono-substituted thiazolones, one–one dimethylthiazole-4,5-dicarboxylate and 1,3-thiazin-4-one, *N*-ferrocenylimino-pyrimidones/imidazolones, one intermediate β-adduct and via oxidative cyclization, a ferrocenyl-1,2,4-triazole. Ring isomerization of 1,3-thiazin-4-ones to a 1,3-thiazolones was detected. The structure of the new compounds was established by IR and NMR spectroscopy, including HMQC, HMBC and DEPT measurements and supported with GIAO NMR calculations and controlled also synthetically by phase-transfer methylation. For three compounds the stereostructure was also proved by X-ray diffraction.

Keywords: Ferrocene; Heterocycles; NMR spectroscopy; X-ray diffraction; S–O and S–N close contact; DFT calculations

1. Introduction

During the last decades the chemistry of ferrocenes has attracted remarkable attention due to their wide range of interest in material sciences and catalysis [1]. Besides these applications the sandwich complexes have also been shown different biological activities and were also used in therapy [2]. Earlier our group have synthesized and characterized different ferrocene-containing heterocycles of potential and – in a few cases [3e] – proved biological activity, including ferrocenyl-pyrazoles- and pyrazolines-, condensed 1,2,4-triazoles- [3], imidazoles- [4], diazepines- [5], oxazoles- [6] and pyridazines [7]. According to the literature different heterocyclic compounds possess valuable pharmaceutic properties including anticancer effects [8–11]. These results prompted us to extend our research to the group of pharmacologically promising ferrocenyl heterocycles, so we decided to prepare two series of novel ferrocene-containing sulfur- and nitrogen heterocycles from the easily available thiosemicarbazones of formyl- and acetylferrocene (**1a**,**b**, Scheme 1) [12] and their *S*-methyl derivatives (**5a**,**b**, Scheme 2), respectively.

2. Results and discussion

For the cyclization of both types of precursors we used dimethyl-acetylene-dicarboxylate (DMAD), a reagent suitable to construct polar azines and azoles carrying at least one carbomethoxy group which provides further possibility for a variety of coupling reactions including e.g. fixation to peptide carriers. Treatment of **1a**,**b** with DMAD in refluxing acetonitrile (Method A) afforded three types of cyclic products (**2**, **3a**,**b**, **4b**, Scheme 1) in moderate to good yields. As the result of conjugate addition of sulfur center and intramolecular *N*-acylation, the corresponding thiazolone (**3a**,**b**) could be isolated as exclusive (**3a**) or major (**3b**) product stabilized by S–O- and S–N close contact interactions [13] involving the other carbomethoxy group in a

* Corresponding authors. Address: Research Group for Protein Modelling, Hungarian Academy of Sciences, Eötvös Loránd University, P.O. Box 32, H-1518 Budapest 112, Hungary. Tel.: +36 1 209 0555; fax: +36 1 209 0602 (P. Sohár).
E-mail address: sohar@para.chem.elte.hu (P. Sohár).

0022-328X/$ - see front matter © 2007 Elsevier B.V. All rights reserved.
doi:10.1016/j.jorganchem.2007.09.017

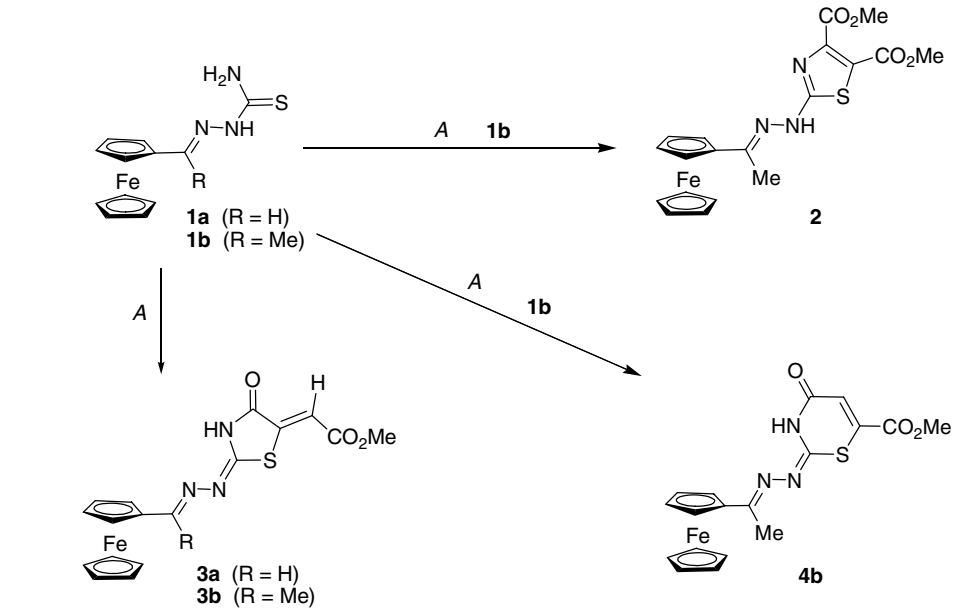

Scheme 1.

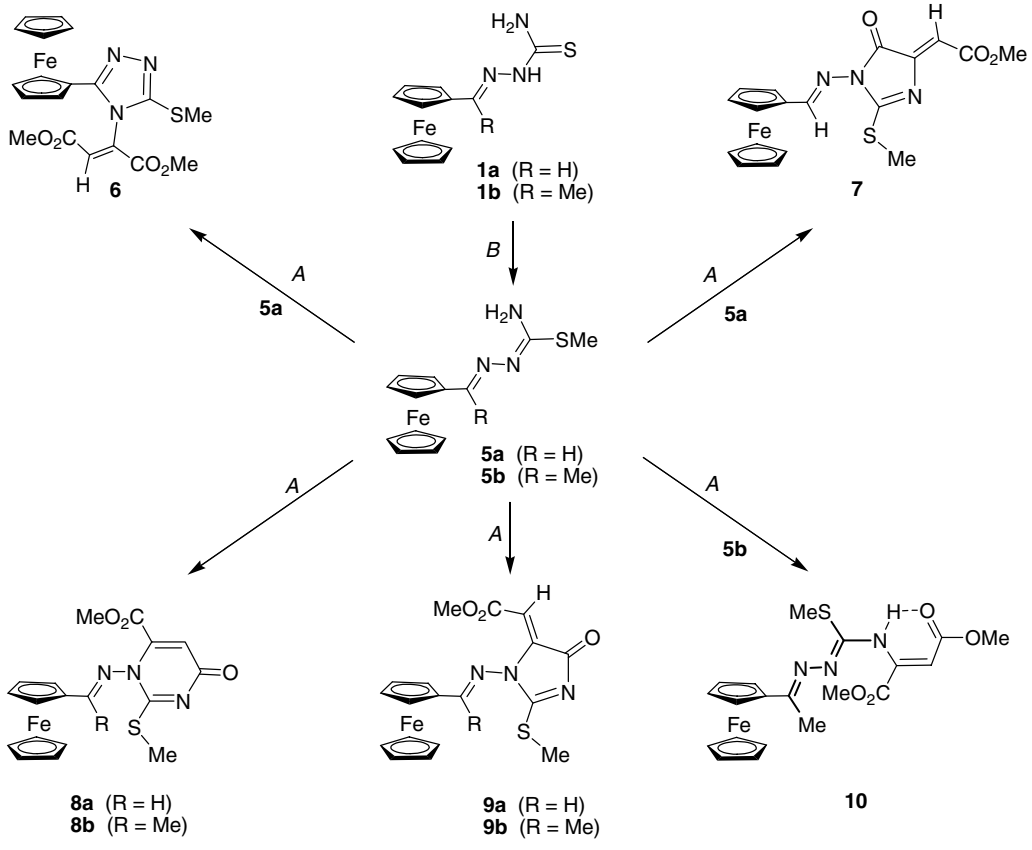

Scheme 2.

quasi-five-membered ring and the imino-nitrogen of the hydrazone moiety in a quasi-four-membered ring, respectively, as evidenced by single crystal X-ray analysis for **3b** (Fig. 1). The reaction of acetylferrocene thiosemicarbazone **1b** gave also two minor products (**2** and **4b**). Dimethylthiazole-4,5-dicarboxylate (**2**) was presumably formed by

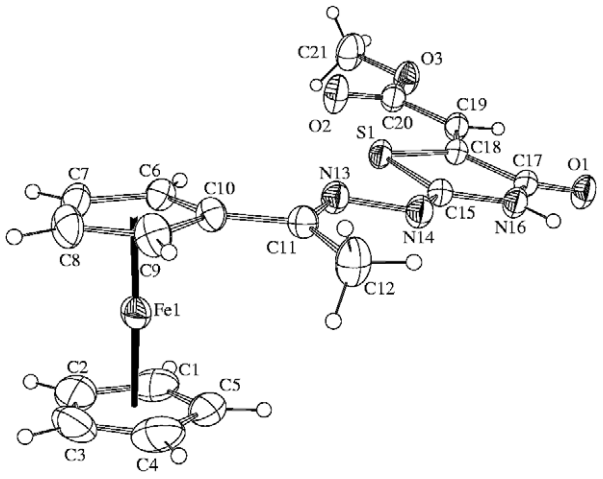

Fig. 1. The ortep diagram of **3b**, only non-hydrogen atoms are labeled, the ellipsoid probability is 30%.

double conjugate addition followed by spontaneous dehydrogenation. The formation of methyl-[1,3]thiazin-4-one-6-carboxylate (**4b**) can be interpreted by conjugate addition of the sulfur center and alternative *N*-acylation presumably furnishing a six-membered ring. As the product ratio **3b**/**4b** increases with longer reaction time, thiazinone **4b** seems to be an instable kinetic product undergoing ring isomerization to **3b** catalyzed by the methanol which is released in the reaction mixture and can cleave the six-membered lactame at elevated temperature. The recyclization of the resulted intermediate involving the methoxycarbonyl group separated by one carbon from the sulfur atom leads to the final product. The relative stability of isomeric pair **3b**/**4b** was estimated by DFT calculations. In keeping with the preparative experiences, the total energy values calculated on the optimized structures *in vacuo* and in MeCN ($\varepsilon = 36.34$) using IEFPCM solvent model [14], respectively, show that **3b** is unambiguously more stable than **4b** [ΔE(**3b**–**4b**) = −24.4 and −26.1 kJ/mol (*in vacuo* and in MeCN, resp.)]. Analogous reactions of benzaldehyde-thiosemicarbazone, thiourea and thionamides affording thiazolones [15] as well as the alternative cyclizations of the same precursors yielding 1,3-thiazin-4-ones [16] have been observed, but the simultaneous formation, interconversion, separation and identification of more products are reported in this paper the first time.

In order to get easily transformable methylthio derivatives, **5a**,**b**, obtained by selective alkylation of **1a**,**b** (Scheme 2), were also reacted with DMAD under the same conditions (Method A). These reactions afforded complex mixtures of methylthio-substituted products in comparable yields including imidazolones and pyrimidones (**7**, **9a**,**b** and **8a**,**b**). From the reaction mixture of **5a** 3-ferrocenyl-4-[(*E*)-1,2-bis(methoxycarbonyl)vinyl]-5-methylthio[1,2,4]-triazole (**6**) could also be isolated as the result of oxidative cyclization associated with conjugate addition on DMAD. A chelate-stabilized enaminoester (**10**) was obtained as an additional product in a considerable yield (32%) from the reaction of **5b**.

The structure elucidation of DMAD-adducts of **1a**,**b** and **5a**,**b** is rather difficult in spite of their relatively small size. Besides two–two regio isomers of open-chain products as **10**, capable of undergoing tautomerization, and the diverse structures containing six- and five-membered rings (as **4b**, **8a**,**b** and **2**, **3a**,**b**, **6**, **7**, **9a**,**b**) together with a few alternative ring constitutions (Fig. 4), *E* or *Z* configuration around the exocyclic C=C bond in the relevant molecules should also be considered.

The structures of **3b**, **8b** and **9b** were proved by X-ray diffraction (Figs. 1–3). The analogous structures of their

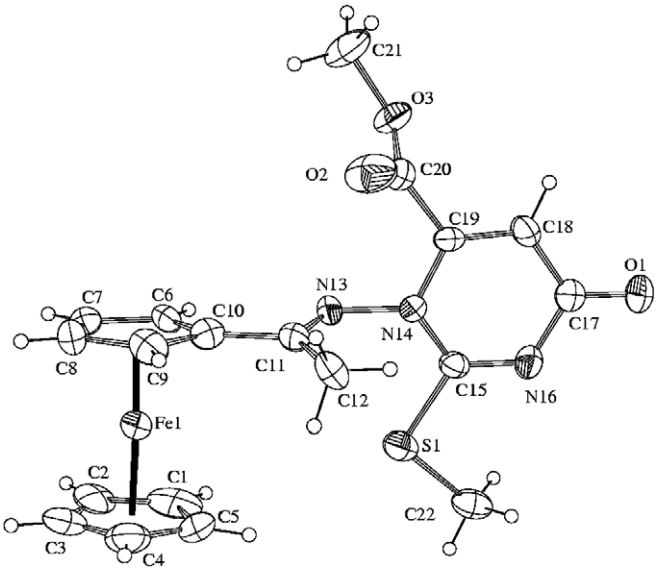

Fig. 2. The ortep diagram of **8b**, only non-hydrogen atoms are labeled, the ellipsoid probability is 30%.

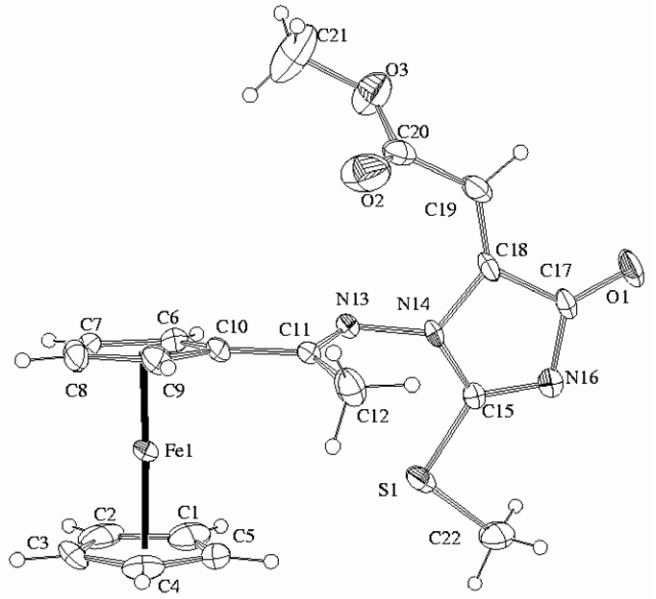

Fig. 3. The ortep diagram of **9b**, only non-hydrogen atoms are labeled, the ellipsoid probability is 30%.

a-type counterparts are straightforward due to very similar ^{1}H and ^{13}C NMR chemical shifts (except for N=CR and C-1′ carbon atoms due to the α- and β-effects [16a], see below).

The ^{1}H and ^{13}C NMR data proving the supposed structures of the new compounds described in this paper are given in Tables 1 and 2. The following additional remarks are necessary:

For **a**–**b** pairs, the α- and β-effects of the methyl group [17a] result in a significant downfield shift of CR and C-1′ lines of the **b**-type compounds (R=Me) as compared to their counterparts **a** (R=H): 5.2–7.5 (for **8a**,**b** 12.0 and for **9a**,**b** 16.1 ppm) and 3.7–4.8 ppm, resp. It is striking that the difference in the shifts of CR for **8a**,**b** and **9a**,**b** pairs is very large! Here, besides the α-effect, the enhanced polarization of the C=N double bond also results in a downfield shift of the *C*Me line due to the electron-withdrawing character of the N atom incorporated in a heterocycle perpendicular to the plane of the directly attached imine group in the most probable rotamer.

For S–C(=N)–N-type carbon in *S*-methyl-thiohydantoine ring (**7** and **9a**,**b**) and thiocarbamide-like moieties (**1a**,**b** and **2**) we measured characteristically downfield shifted signals (171–185 ppm) in accord with literature data [17b].

The ^{1}H NMR signal of the CH=N–X group is downfield shifted (8.34 and 8.25 ppm for **4a** and **5a**) if X=N(sp^2) as compared to X–NH cases (**1a**, 7.86 ppm) due to the anisotropy of the N(sp^2) atom [17c]. In **8a** and **9a** the downfield position of the ^{1}H NMR signal of the CH=N group can be explained by the anisotropy of the S-atom [17d]. Depending on the conformation, a similar interaction may also act in **7** arising from the anisotropic neighboring effect of the carbonyl group [17e].

Due to the crowded structure of **8b** and **9b**, the free rotation of the ferrocenyl group is hindered and as a consequence, the H/C-2′ and H/C-5′ signals and for **8b** also the H/C-3′ and H/C-4′ ones appear separated.

The different shifts of the two NH_2 hydrogens in **1a**,**b** are probably the consequence of a eight-membered dimeric association of the thioamide group in which one of these two H's is involved [18].

The downfield shift of the lactame C=O line of **9a**,**b** by 7.0 ppm (174.2 and 174.8) as compared to **8a**,**b** is due to the five-membered ring structure, while the analogous shifts for **10** is probably the consequence of the positive polarization of the carbonyl carbon in the terminal ester group originating from a chelate-like H-bond.

In order to get further supporting information for the postulated structures **2** and **4b** we calculated the ^{13}C NMR chemical shifts for two series of alternative structures (**2**, **I**, **II** and **4b**, **III**, **IV**, **V**, resp., Fig. 4) by DFT GIAO [19] model at B3LYP/6-311+G(2d,p) level [20] on the structures optimized by B3LYP/6-31G(d) method. All computations were run by GAUSSIAN program package [21]. Only the most diagnostic ^{13}C NMR shifts (relative to TMS-resonance calculated at the same level of DFT) are listed in Tables 3 and 4 together with the measured values. The comparison of the values obtained as the sum of differences between the shifts measured and calculated for a particular carbon gives reliable basis for the correct structures.

The large difference between the shifts of the two vicinal carbons in the heterocyclic ring in **2** (119.0 and

Table 1
^{1}H NMR data[a] of compounds **1a**,**b**, **2**, **3a**–**c**, **4b**, **5a**,**b**, **6**, **7**, **8a**,**b**, **9a**,**b** and **10**[b]

Compound	SCH_3 *s* (3H)	OCH_3 *s* (3H)	N=CR *s* (1/3H)[c]	H-2′,5′ (2H) Substituted *c*-pentane	H-3′,4′ (2H)	H-1″–5″ *s* (5H)[d]	C=CH *s* (1H)	NH_2 (2H)	NH (1H)
1a	–	–	7.86	4.69	4.38	4.17	–	7.56, 7.98	11.13
1b	–	–	2.18	4.78	4.35	4.16	–	7.64, 8.08	9.93
2	–	3.86, 3.95	2.15	4.64	4.38	4.17	–	–	~9.15
3a	–	3.78	8.34	4.71	4.53	4.22	6.64	–	
3b	–	3.76	2.28	4.72	4.46	4.18	6.61	–	
3c	3.38[e]	3.83	2.40	4.81	4.54	4.25	6.77	–	–
4b	–	3.85	2.32	4.71	4.42	4.19	6.33	–	~9.6
5a	2.51	–	8.25	4.64	4.39	4.22	–	5.40	–
5b	2.50	–	2.33	4.67	4.33	4.17	–	5.25	–
6	2.80	3.82, 4.00	–	4.87	4.35	4.12	6.47	–	–
7	2.72	3.86	8.42	4.77	4.63	4.31	5.90	–	–
8a	2.57	3.89	8.37	4.82	4.69	4.42	6.50	–	–
8b	2.52	3.84	2.23	4.77, 4.83	4.59	4.35	6.50	–	–
9a	2.72	3.65	8.28	4.73	4.58	4.34	6.18	–	–
9b	2.70	3.51	2.30	4.66, 4.91	4.52, 4.54	4.31	6.07	–	–
10	2.56	3.77, 3.79	2.18	4.71	4.35	4.14	5.54	–	9.86

[a] In DMSO-d_6 (**1a**,**b**, **3a**–**c**, **8a**,**b**, **9a**,**b** and **10**) or $CDCl_3$ solution (**2**, **4b**, **5a**,**b**, **6** and **7**) at 500 MHz. Chemical shifts in ppm ($\delta_{TMS} = 0$ ppm).
[b] Assignments were supported by HMQC measurements (for **3a**–**c**, **4b**, **6**, **7**, **8a**, **9b** and **10**), HMBC (for **1a**,**b**, **2**, **3c**, **5a**) and DIFFNOE (for **8a**,**b** and **9a**,**b**).
[c] R = H (CH_3 for **2**, **3c**, **10** and **b**-type compounds).
[d] Unsubstituted cyclopentadiene ring.
[e] NMe group.

Table 2
^{13}C NMR chemical shifts[a] of compounds **1a**,**b**, **2**, **3a**–**c**, **4b**, **5a**,**b**, **6**, **7**, **8a**,**b**, **9a**,**b** and **10**[b]

Compound	SCH_3	CCH_3	C=O ester	C=O ring	C=*C*H	=C– *quat.*	OCH_3[c]	N=CH or N=CCH_3	=C–S or C=S	C-1′ Substituted	C-2′,5′ *Cp* ring	C-3′,4′	C-1″–5″ Unsubstituted *Cp*
1a	–	–	–	–	–	–	–	144.2	177.8	79.8	68.5	70.9	69.8
1b	–	15.9	–	–	–	–	–	151.5	178.9	84.0	68.1	70.6	69.9
2	–	14.8	161.5	163.7[d]	119.0[e]	148.2[f]	52.8	151.7	171.2	82.6	67.5	70.8	69.8
3a	–	–	166.9[g]	166.8[g]	114.7	144.1	53.3	160.9	157.9	78.5	69.3	72.0	70.1
3b	–	16.8	166.9[h]	166.9[h]	114.3	144.7	53.2	166.1	157.6	82.9	68.4	70.3	70.2
3c	30.5[i]	16.7	166.8	165.3	115.1	143.1	53.3	167.5	156.8	82.7	68.5	71.4	70.2
4b	–	16.6	165.6	164.0	121.6	133.3	53.1	166.8	154.0	82.2	68.3	71.1	70.0
5a	13.2	–	–	–	–	–	–	155.2	160.3	79.9	68.5	70.6	69.6
5b	13.1	16.0	–	–	–	–	–	161.1	158.3	84.6	67.6	70.2	69.7
6	17.0	–	162.6	165.3[d]	111.2	140.6	52.7	164.6	156.4	74.1	68.4	70.1[h]	70.1[h]
7	15.2	–	164.9	170.5	105.4	138.6	53.0	168.2	181.0	75.2	69.7	73.0	70.4
8a	14.8	–	160.5	167.2	111.4	141.0	53.6	175.1	163.4	73.6	70.0	73.1	69.9
8b	14.9	18.4	160.7	167.8	111.4	141.6	53.8	187.1	163.1	78.4	69.0, 69.6	72.7	70.4
9a	15.5	–	164.8	174.2	103.3	136.4	52.6	169.1	185.0	75.2	69.6	72.6	70.2
9b	15.3	18.6	164.5	174.8	103.2	137.8	52.4	185.2	184.6	79.1	67.9, 70.3[h]	72.1, 72.5	70.3[h]
10	13.8	16.2	164.9	170.0[d]	99.1	147.0	52.2	164.0	154.5	83.3	68.1	70.7	69.8

[a] In DMSO-d_6 (**1a**,**b**, **3a**–**c**, **8a**,**b**, **9a**,**b**, **10**) or $CDCl_3$ solution (**2**, **4b**, **5a**,**b**, **6**, **7**) at 125 MHz. Chemical shifts in ppm ($\delta_{TMS} = 0$ ppm).
[b] Assignments were supported by DEPT (except for **1a**, **3c**, **6**, **7**, **9a**, **10**), HMQC (for **3a**–**c**, **4b**, **6**, **7**, **8a**, **9b**, **10**) and HMBC (except for **1a**,**b**, **2**, **5a**) measurements.
[c] For compounds containing two OCH_3 groups appear the second line at: 53.3 (**2**), 53.8 (**6**), 53.0 (**10**).
[d] Ester group, on C, ß-to N (**2, 6**,**10**).
[e/f] C-5/4 lines, thiazole ring.
[g] Interchangeable assignments.
[h] Overlapping lines.
[i] N-CH_3 group.

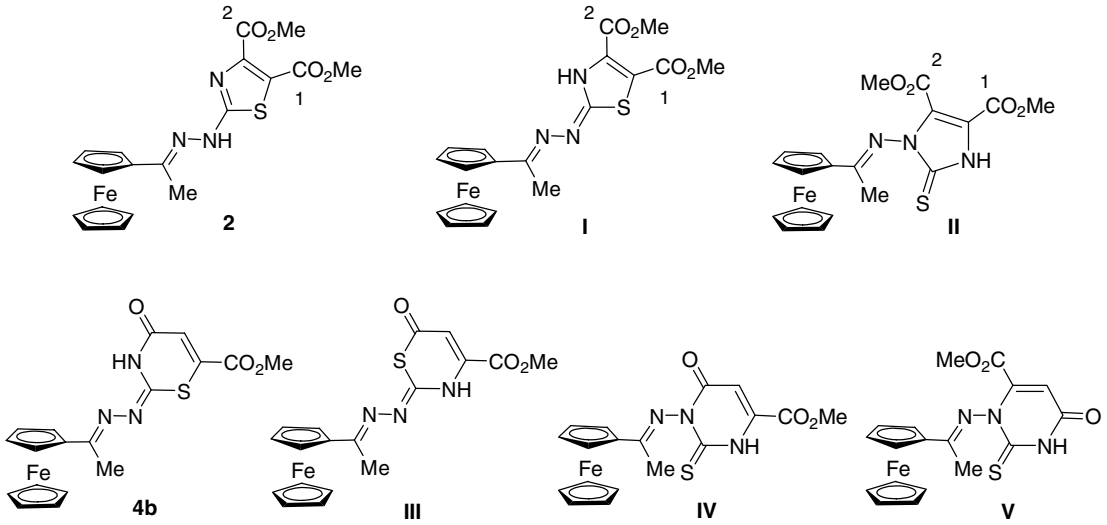

Fig. 4. Two sets of possible structures (**2**, **I**, **II** and **4b**, **III**, **IV**, **V**, resp.) analyzed by DFT GIAO NMR calculations at B3LYP/6-311+G(2d,p) level of theory. The numbering of CO_2Me groups in **2**, **I** and **II** is used in Table 3.

148.2 ppm) excludes the imidazoline-thione ring containing structure **II**. Among the two tautomers of the thiazole derivatives **2** and **I**, the heteroaromatic **2** is chemically *ab ovo* more probable. The very similar chemical shifts of CMe in **2** and **1b** (151.7 and 151.5 ppm) and also the calculated carbon shifts for **2**, **I** and **II** supported the thiazole structure **2**. The sum of differences between the measured and calculated values (cf. Table 3) is double for **I** and **II** than for **2**.

Since the comparison of measured and calculated carbon shifts for **4b** together with the relevant data computed for structures **III**–**V** (Table 4) provides less convincing evidences for the assumed structure (cf. the smaller differences in the sum of deviations), we attempted methylation of **4b** under mild phase-transfer conditions (Scheme 3, Method C). On the basis of the shifts of ring carbons being very similar to those measured for **3b** and the HMBC results, the product was assigned as **3c** (Scheme 3). In a control

Table 3
Characteristic ^{13}C NMR shifts of **2** and its alternative structures **I**–**II** (cf. Fig. 4) calculated by B3LYP/6-311+G(2d,p) using GIAO model (reference: TMS)

	Fc–*C*=N	*C*–S_{ring} *C*–NH^{a}_{ring}	*C*–N_{ring} *C*–N–N^{a}_{ring}	S–*C*=N N–*C*(S)–N[a]	$CO_2Me(1)$	$CO_2Me(2)$	Me	$\sum_{deviation}$
Measured	151.8	119.0	148.2	171.4	163.7	161.5	14.8	0
Calc. (**2**)	150.4	126.2	156.4	177.9	171.7	167.3	12.1	**34.0**
Calc. (**I**)	166.7	131.1	135.8	167.7	169.2	168.8	14.2	60.6
Calc. (**II**)	188.9	120.8	135.9	169.4	165.9	163.0	18.6	62.9

[a] For structure **II**.

Table 4
Characteristic ^{13}C NMR shifts of **4b** and its alternative structures **III**–**V** (cf. Fig. 4) calculated by B3LYP/6-311+G(2d,p) using GIAO model (reference: TMS)

	Fc–*C*=N	*C*H_{ring}	*C*=O_{ring}	*C*CO_2Me	N–*C*=N S–*C*=N	*C*O_2Me	Me	CO_2*Me*	$\sum_{deviations}$
Measured	166.8	121.6	164.0	133.3	154.0	165.6	16.6	53.1	0
Calc. (**4b**)	172.5	128.9	165.9	155.9	162.1	171.8	14.1	55.2	**55.2**
Calc. (**III**)	172.7	105.1	190.2	144.2	164.2	172.6	14.2	55.6	81.6
Calc. (**IV**)	196.2	113.3	162.0	152.6	182.0	170.8	19.7	55.0	97.1
Calc. (**V**)	187.4	110.7	162.4	141.7	180.9	170.6	17.1	55.7	76.3

experiment **3b** also afforded **3c** under the same conditions. The ring transformation of type **4** → **3** probably takes place by the initial cleavage of the *N*-methylated lactame **4c** effected by the excess of hydroxide anion. The carboxylate anion formed upon the ring opening is methylated by the excess of iodomethane and the resulting fumarate intermediate **11** undergoes ring closure affording **3c**. It seems that the ring opening step must be preceeded by primary *N*-methylation, and prevented in the recoverable **4b**, which exists mainly in deprotonated form in the basic reaction mixture. This type of conversion is closely related to the above discussed transitional formation and subsequent ring transformation of **4b**.

The conversion discussed above gives an unambiguous preparative evidence for the presence of 5-methoxycarbonyl-1,3-thiazin-4-one moiety in **4b**, ruling out the possibility of structures **III**–**V**.

The X-ray single crystal analysis of **3b**, **8b** and **9b** revealed their structures depicted in Figs. 1–3. The data collection and crystallographic parameters are summarized in Table 5.

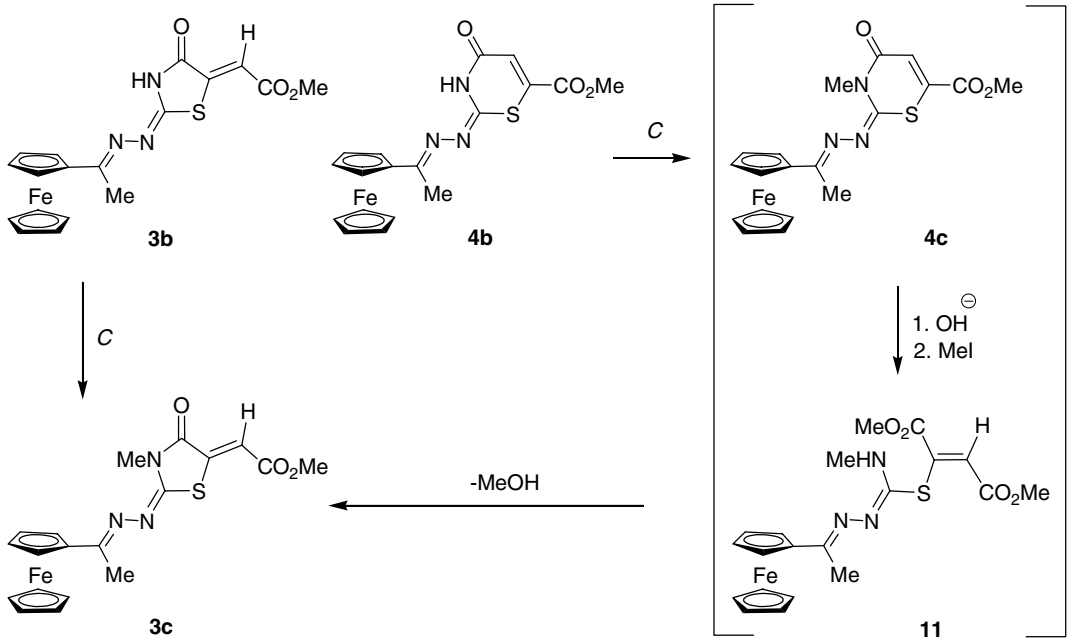

Scheme 3.

The molecular structure of **3b** is nearly planar except for the ferrocenyl block, the rms of the least-squares plane is 0.145. The interatomic distances between the O2–S1 and N13–S1 atom pairs [2.840(2) and 2.808(2) Å, resp.] are shorter than the sum of thei appropriate van der Waals radii, referring to S–X close contact interactions [13].

Apart from the size of the incorporated heterocycles the other two structures (**8b** and **9b)** show much similarity. Avoiding steric crowdance in both molecules the ferrocenylimino- and heterocyclic units are in twisted conformation, their planes being nearly perpendicular relative to each other. The angle between the least-squares plane of the substituted *Cp* rings and the heterocycles are 78.5(2)° and 82.9(3)° in **8b** and **9b**, respectively. The carbomethoxy group is situated in *exo* position relative to the ferrocenyl group and the S1 atom of the methylthio substituent is directed towards the *endo* position of the ferrocenyl group. The carbomethoxy group turns out of the plane of the imidazole or pyrimidine ring, the least-squares planes angles are 64.6(4)° and 68.0(4)° in **9b** and **8b**, respectively. The least-squares planes of the central nitrogen containing and C6–C7–C8–C9–C10 Cp rings are nearly perpendicular; they have a setting angle of 78.5(2)° in **9b** and 82.9(3)° in **8b**. In both structures the two Cp rings (C1–C2–C3–C4–C5 and C6–C7–C8–C9–C10) are parallel, the plane angle between them is 2.2(7)° in **8b** and 2.3(5)° in **9b**. The Fe atom is 1.643(3) and 1.641(3) Å above them, respectively. The conformation of the ferrocene in this molecule is eclipsed.

The main crystal building forces are in all compounds the classical N–H···O hydrogen bonds and the C–H···N and C–H···O interactions. The crystal structure of **3b** is much different from the others, it has a smaller unit cell with $P\bar{1}$ space group. The hydrogen bonded centrosymmetric dimers form a plane through C–H···O interactions (H21A to O1 and H19 to O3). Between these planes there are π–π stacking interactions (thiazoline and non-substituted *Cp* rings). The crystal structures of the other two

Table 5
Data collection and crystallographic parameters

Compound	**3b**	**8b**	**9b**
Crystal data			
Empirical formula	$C_{18}H_{17}FeN_3O_3S$	$C_{19}H_{19}FeO_3N_3S$	$C_{19}H_{19}FeO_3N_3S$
Formula weight	441.3	425.28	425.28
Crystal color, habit	Red, chunky	Red, needle	Red, needle
Crystal dimensions (mm)	$0.99 \times 0.45 \times 0.41$	$0.60 \times 0.40 \times 0.10$	$0.30 \times 0.30 \times 0.20$
Crystal system	Triclinic	Monoclinic	Monoclinic
Space group	$P\bar{1}$	$P2_1/n$	$P2_1/n$
Lattice parameters			
a (Å)	8.262(3)	11.710(6)	11.117(2)
b (Å)	10.233(3)	9.583(1)	10.178(2)
c (Å)	12.017(3),	17.61(2)	17.322(2)
α (°)	71.32(1)		
β (°)	70.35(1)	104.91(4)	104.23(1)
γ (°)	80.03(1)		
Volume (Å^3)	904.1(5)	1910.5(2)	1899.7(5)
Z-Value	2	4	4
D_{calc} (g cm^{-3})	1.511	1.479	1.487
Data collection			
Diffractometer	Rigaku R-AXIS RAPID	Rigaku AFC6S	Rigaku AFC6S
Radiation type	Mo Kα, 0.71070	Cu Kα, 1.54178	Cu Kα, 1.54178
Absorption coefficient (mm^{-1})	0.980	7.565	7.606
$F(000)$	440	880	880
Index ranges	$-10 \leqslant h \leqslant 10$ $-13 \leqslant k \leqslant 13$ $-15 \leqslant l \leqslant 15$	$-14 \leqslant h \leqslant 14$ $-12 \leqslant k \leqslant 12$ $-22 \leqslant l \leqslant 22$	$-13 \leqslant h \leqslant 13$ $-12 \leqslant k \leqslant 12$ $-21 \leqslant l \leqslant 21$
Reflections collected	43276	8884	7700
Independent reflections	4125	4109	3670
R_{int}	0.0314	0.1388	0.1439
Refinement			
Model/parameters	4159/235	3753/245	3670/245
R indices [$I > 2\sigma(I)$]	$R_1 = 0.0388$, $wR_2 = 0.1085$	$R_1 = 0.0689$, $wR_2 = 0.1370$	$R_1 = 0.0633$, $wR_2 = 0.1316$
R indices (all data)	$R_1 = 0.0460$, $wR_2 = 0.1125$	$R_1 = 0.2156$, $wR_2 = 0.2065$	$R_1 = 0.1800$, $wR_2 = 0.1715$
Extinction coefficient	–	0.0011(2)	0.0048(4)
Largest difference in peak and hole (e Å^{-3})	0.73 and −0.24	0.43 and −0.59	0.47 and −0.84

Table 6
Hydrogen bonds in the crystals of **3b**, **8b** and **9b**

	Donor–H···acceptor	*d*(D–H)	*d*(H···A)	*d*(D···A)	∠(D–H···A)
3b	N16–H16···O1[a]	0.86	2.02	2.844(2)	161.4
	C19–H19···O3[b]	0.93	2.70	3.588(3)	160.8
	C21–H21A···O1[b]	0.96	2.59	3.531(4)	168.6
8b	C22–H22C···N13[c]	0.96	2.68	3.426(10)	135.1
	C6–H6···N16[c]	0.93	2.72	3.625(9)	165.3
	C19–H19···O1[d]	0.93	2.43	3.263(7)	149.3
9b	C21 – H21A···O1[e]	0.96	2.71	3.084(11)	103.9
	C22–H22C···N13[f]	0.96	2.69	3.379(12)	129.3

Translation of symmetry-codes to equivalent positions:
[a] $-x, -y+1, -z$; [b] $-x+1, -y, -z$; [c] $-x, -y+1, -z$; [d] $-x+1, -y+1, -z$; [e] $x, y-1, z$; [f] $-x, -y+1, -z$.

compounds (**8b** and **9b**) are isomorphs. The unit cells are very similar and both space group is $P2_1/n$. The small differences in the molecular structure causes that different atoms get closer, so different hydrogen bonding pattern is realized (see Table 6). The distinct layers of the apolar ferrocenyl and the polar other moieties run parallel to the *ab* plane of the unit cell.

The optimized structure of **3b** obtained by B3LYP/6-31G(d) level of DFT is in acceptable accord with that revealed by X-ray analysis and exhibits a nearly coplanar arrangement of the planes of thiazolone and the Cp ring of ferrocene ($\Theta = 5.7°$). The computed S–O and S–N close contact interactions are similar to the measured interatomic distances ($d_{S-O}/d_{S-N} = 2.863$ Å/2.873 Å *vs.* the measured values: $d_{S-O}/d_{S-N} = 2.841(2)$ Å/2.808(2) Å). The geometry optimization performed at enhanced B3LYP/6-31G(2d) level afforded a structure with slightly shorter interatomic distances ($d_{S-O}/d_{S-N} = 2.858$ Å/2.864 Å), which are closer to the measured ones. The geometry optimization carried out for **4b** at B3LYP/6-31G(d) level of theory also led to a structure containing the thiazinone ring nearly coplanar with the Cp ring of ferrocene ($\Theta = 4.8°$), and stabilized by pronounced S–O and S–N close contact interactions ($d_{S-O}/d_{S-N} = 2.863$ Å/2.748 Å). It is worth to note that the calculated S–O distance in a quasi-four membered ring in **4b** is exactly identical with that resulted for **3b** containing the interaction in a quasi-five membered ring. In the structure optimized for **2** at B3LYP/6-31G(d) level, the planes of the thiazole- and Cp rings are also nearly coplanar ($\Theta = 6.7°$), but the sulfur atom involved in the aromatic ring is less capable of establishing interactions with non-directly bonded donor atoms ($d_{S-O}/d_{S-N} = 3.017$ Å/2.980 Å).

3. Conclusion

Besides DMAD employing further activated acetylene components the extension of the discussed simple cyclization reactions of the easily available ferrocenyl-thiosemicarbazones and their *S*-methylated derivatives can be used for the synthesis of a variety of novel ferrocenyl-substituted S,N- and N,N-heterocycles of potential biological interest. By the choice of the appropriate precursor, the sulfur atom can be incorporated in the ring or in the alkylthio substituent. The intramolecular S–O and S–N close contact interactions seem to be governing factors in the cyclization reactions of thiosemicarbazone-reagents. By increasing the polarity of the imino moiety the strongly electron-donating ferrocenyl group may contribute to the development of the stabilizing S–N close contact. The high-level DFT calculation and comparison of ^{13}C NMR chemical shifts for the possible sets of isomers may serve as a useful supplementary tool in finding the correct structure of a heterocycle with low number of attached hydrogen atoms.

4. Experimental

4.1. General

Melting points were determined with a Boethius microstage and are uncorrected. The IR spectra were run in KBr disks on a Bruker IFS-55 FT-spectrometer controlled by Opus 3.0 software. The ^1H and ^{13}C NMR spectra were recorded in $CDCl_3$ solution in 5 mm tubes at RT, on a Bruker DRX-500 spectrometer at 500.13 (^1H) and 125.76 (^{13}C) MHz, with the deuterium signal of the solvent as the lock and TMS as internal standard. The standard Bruker microprogram NOEMULT to generate NOE [22] and to get DIFF-NOE spectra [17f,23] was used with a selective pre-irradiation time. DEPT spectra [24] were run in a standard manner [25], using only a $\Theta = 135°$ pulse to separate the CH/CH_3 and CH_2 lines phased "up" and "down", respectively. The 2D-COSY [26a,27a], HMQC [26b,27b] and HMBC [28,29] spectra were obtained by using the standard Bruker pulse programs.

The summary of crystallographic data for **3b**, **8b** and **9b** is compiled in Table 5.

An irregular chunky crystal of **3b** of $0.99 \times 0.45 \times 0.41$ mm size was mounted in a loop on a Rigaku R-AXIS RAPID IP area detector diffractometer ($T = 295$ K) using graphite monochromated Mo Kα radiation from a sealed tube operating at 50 kV 36 mA. 36 Frames in 180° slices (5° image width in omega) were collected in six scans at chi = 0 and chi = 54°, respectively. Integration (FS process, T. Higashi) of these frames gave 43 276 reflections of which 4125 proved to be unique ($R_{int} = 0.0314$). Initial structure model obtained by the use of SHELXS-97 [30] gave most of the non-hydrogen atoms, rest of which were subsequently located and refined to their final positions via full-matrix least squares (SHELXL-97 [31]) following standard procedures.

The crystals of **8b** and **9b** were mounted on a glass fiber. These measurements were made on a Rigaku AFC6S diffractometer with graphite monochromated Cu Kα radiation ($\lambda = 1.54178$ Å). Cell constants and orientation matrix for data collection were obtained from a least-squares refinement using the setting angles of carefully centered reflections. The data were collected a temperature of 293 K using the $\omega/2\theta$ scan technique. Backgrounds were

measured in half the total time of peak scans. The intensities of three representative reflections were monitored after every 150 reflections. No decay correction was applied. The data were corrected for Lorentz and polarization effects.

For **9b** a total of 7700 reflections were collected of which 3670 were unique [$R_{int} = 0.1439$]. For **8b** of the 7878 reflections which were collected 4054 were unique [$R_{int} = 0.1853$]. The linear absorption coefficient, μ, for Cu Kα radiation is 1.685 mm^{-1} for **9b** and 1.337 mm^{-1} for **8b**. An empirical absorption correction [32] was applied to the data.

Data processing was carried out using the software supplied with the diffractometer. The initial structure model was obtained from heavy atom Patterson methods [33] for **8b** and direct methods [34] for **9b**. The non-hydrogen atoms were refined anisotropically. Hydrogen atoms were generated based upon geometric evidence and their positions were refined by the riding model. All calculations were performed using the teXsan [35] crystallographic software package of Molecular Structure Corporation except for refinement, which was performed using SHELXL-97 [31] with full-matrix least-squares method on F^2.

Thiosemicarbazones **1a**,**b** and were prepared according to described procedure [12].

4.2. General procedure for the synthesis of compounds 5a,b (Method B)

The corresponding thiosemicarbazone (**1a**,**b**, 10 mmol) and iodomethane (1.42 g, 10 mmol) were added to the solution obtained by dissolving 0.23 g (10 mmol) sodium in methanol (50 mL). The reaction mixture was stirred and refluxed under Ar for 1 h. The solvent was evaporated to dryness, and the solid residue was purified by column chromatography on silica, using DCM as eluent. The products were crystallized from *n*-hexane or *n*-hexane–ethanol (10:1).

4.2.1. (1Z)-1-(Ferrocenylmethylideneamino)-2-methylisothiourea (5a)

Orange powder; yield: 91%; mp 99–101 °C; Anal. Calc. for $C_{13}H_{15}FeN_3S$ (301.20): C, 51.84; H, 5.02; N, 13.95. Found: C, 53.40; H, 5.12; N, 13.81%.

4.2.2. (1Z)-1-(1-Ferrocenylethylideneamino)-2-methylisothiourea (5b)

Orange powder; yield: 85%; mp 83–84 °C; Anal. Calc. for $C_{14}H_{17}FeN_3S$ (315.22): C, 53.35; H, 5.44; N, 13.33. Found: C, 53.11; H, 5.50; N, 13.73%.

4.3. General procedure for the reactions with DMAD (Method A)

The mixture of the corresponding thiosemicarbazone- or methylthio derivative (**1a**,**b** or **5a**,**b**: 4 mmol) and DMAD (0.711 g, 5 mmol) was dissolved in anhydrous MeCN (50 mL). The solution was refluxed under Ar for 1–3 h (**1a**,**b**) or 3 h (**5a**,**b**) then evaporated to dryness. The solid residue was triturated with *n*-hexane and filtered off to remove the excess of DMAD. The deep orange powder was dissolved in DCM (50 mL) and extracted with water (3×50 mL). The organic phase was dried (Na_2SO_4) and evaporated. The residue was chromatographed over silica using *n*-hexane or different mixtures of *n*-hexane–EtOAc as eluent. The separated products were crystallized from *n*-hexane.

4.3.1. Dimethyl 2-[(E)-2-(1-ferrocenylethylidene)-hydrazinyl]thiazole-4,5-dicarboxylate (2)

Red powder; yield: 0.229 g, 13% (reaction time: 1 h) 0.176 g, 10% (reaction time: 3 h); mp 182–184 °C; Anal. Calc. for $C_{19}H_{19}FeN_3O_4S$ (441.28): C, 51.71; H, 4.34; N, 9.52; S, 7.27. Found: C, 51.93; H, 4.46; N, 9.71; S, 7.16%.

4.3.2. (2Z)-Methyl 2-{(2Z)-2-[(E)-2-(ferrocenylmethylidene)hydrazono]-4-oxothiazol-idin-5-ylidene}acetate (3a)

Red powder; yield: 1.223 g, 77% (reaction time: 1 h); mp 232–240 °C; Anal. Calc. for $C_{17}H_{15}FeN_3O_3S$ (397.23): C, 51.40; H, 3.81; N, 10.58; S, 8.07. Found: C, 51.41; H, 4.01; N, 10.12; S, 7.96%.

4.3.3. (2Z)-Methyl 2-{(2Z)-2-[(E)-2-(1-ferrocenylethylidene)hydrazono]-4-oxothiazol-idin-5-ylidene}acetate (3b)

Red powder; yield: 0.460 g, 28% (reaction time: 1 h), 0.872 g, 53% (reaction time: 3 h); mp 211–214 °C; Anal. Calc. for $C_{18}H_{17}FeN_3O_3S$ (411.27): C, 52.57; H, 4.17; N, 10.22; S, 7.80. Found: C, 52.35; H, 4.25; N, 10.12; S, 7.95%.

4.3.4. (2E)-Methyl 2-[(E)-2-(1-ferrocenylethylidene)-hydrazono]-3,4-dihydro-4-oxo-2H-1,3-thiazone-6-carboxylate (4b)

Red powder; yield: 0.740 g, 45% (reaction time: 1 h), 0.164 g, 10% (reaction time: 3 h); mp 134–137 °C; Anal. Calc. for $C_{18}H_{17}FeN_3O_3S$ (411.27): C, 52.57; H, 4.17; N, 10.22; S, 7.80. Found: C, 52.43; H, 4.22; N, 10.08; S, 7.88%.

4.3.5. Dimethyl 2-(3-ferrocenyl-5-(methyltho)-4H-1,2,4-triazol-4-yl)fumarate (6)

Deep red powder; yield: 0.353 g, 20%; mp 127–29 °C; Anal. Calc. for $C_{19}H_{19}FeN_3O_4S$ (441.29): C, 51.71; H, 4.34; N, 9.52; S, 7.27. Found: C, 51.57; H, 4.38; N, 9.42; S, 7.32%.

4.3.6. (2Z)-Methyl 2-[1-(ferrocenylmethylideneamino)-2-(methylthio)-5-oxo-1H-imidazol-4(5H)-ylidene]acetate (7)

Red powder; yield: 0.576 g, 35%; mp 122–24 °C; Anal. Calc. for $C_{18}H_{17}FeN_3O_3S$ (411.27): C, 52.57; H, 4.17; N, 10.22; S, 7.80. Found: C, 52.61; H, 4.10; N, 10.04; S, 7.82%.

4.3.7. Methyl 3-(ferrocenylmethylideneamino)-3,6-dihydro-2-methylthio-6-oxopyrimidine-4-carboxylate (8a)

Orange powder; yield: 0.329 g, 20%; mp 132–35 °C, Anal. Calc. for $C_{18}H_{17}FeN_3O_3S$ (411.27): C, 52.57; H,

4.17; N, 10.22; S, 7.80. Found: C, 55.72 H 4.38; N, 10.62; S, 7.90%.

*4.3.8. Methyl 3-(ferrocenylethylideneamino)-3,6-dihydro-2-methylthio-6-oxopyrimidine-4-carboxylate (**8b**)*

Orange powder; yield: 0.510 g, 30%; mp 112–116 °C, Anal. Calc. for $C_{19}H_{19}FeN_3O_3S$ (425.29): C, 53.66; H, 4.50; N, 9.88; S, 7.54. Found: C, 53.75; H, 4.54; N, 9.85; S, 7.59%.

*4.3.9. (2E)-Methyl [2-(1-ferrocenylmethylideneamino)-2-methylthio-4-oxo-1H-imidazol-5(4H)-ylidene]acetate (**9a**)*

Red powder; yield: 0.247 g, 15%; mp 143–45 °C; Anal. Calc. for $C_{18}H_{17}FeN_3O_3S$ (411.27): C, 52.57; H, 4.17; N, 10.22; S, 7.80. Found: C, 52.60; H, 4.26; N, 10.11; S, 7.84%.

*4.3.10. (2E)-Methyl [2-(1-ferrocenylethylideneamino)-2-methylthio-4-oxo-1H-imidazol-5(4H)-ylidene]acetate (**9b**)*

Red powder; yield: 0.306 g, 18%; mp 159–61 °C; Anal. Calc. for $C_{19}H_{19}FeN_3O_3S$ (425.29): C, 53.66; H, 4.50; N, 9.88; S, 7.54. Found: C, 53.52; H, 4.68; N, 9.96; S, 7.48%.

*4.3.11. Dimethyl 2[(1Z)-(1-ferrocenylethylideneamino)-2-methylisothioureido]fumarate (**10**)*

Orange powder; yield: 0.585 g, 32%; mp 138–140 °C, Anal. Calc. for $C_{20}H_{23}FeN_3O_4S$ (457.34): C, 52.53; H, 5.07; N, 9.19; S, 7.01. Found: C, 53.58; H, 5.18; N, 9.27; S, 6.96%.

*4.4. Phase-transfer methylation of **3b** and **4b** (Method C)*

To the stirred suspension of **3b** or **4b** (0.411 g, 1mmol) in DCM (25 mL) 1 M methanolic solution of Bu_4NOH (2.5 mL, 2.5 mmol) and subsequently iodomethane (0.568 g, 4 mmol) were added under Ar at 25 °C. The clear deep red solution, formed after 20–30 min of stirring at 25 °C, was evaporated. The residue was triturated with a small amount of cold EtOH, then filtered off and dissolved again in DCM (5 mL). The solution was chromatographed on silica using DCM as eluent to separate **3c** from the unreacted portion of **3b** or **4b** which were isolated by the collection and evaporation of the second band. The evaporation of the solution of the first fraction afforded **3c** which was recrystallized by a small amount of EtOH.

*4.4.1. (2Z)-Methyl 2-{(2Z)-2-[(E)-2-(1-ferrocenylethylidene)hydrazono]-3-methyl 4-oxothiazolidin-5-ylidene}acetate (**3c**)*

Red powder; yield: 0.332 g, 71% (from **3b**) and 0.089 g, 21% (from **4b**); mp 174–175 °C; Anal. Calc. for $C_{19}H_{19}FeN_3O_3S$ (425.28): C, 53.66; H, 4.50; N, 9.88; S, 7.54. Found: C, 53.76; H, 4.43; N, 10.02; S, 7.45%.

5. Supplementary material

CCDC 294707, 294706 and 294705 contain the supplementary crystallographic data for **3b**, **8b** and **9b**. These data can be obtained free of charge from The Cambridge Crystallographic Data Centre via www.ccdc.cam.ac.uk/data_request/cif.

Acknowledgements

This work was supported by the Hungarian Scientific Research Fund (OTKA T-043634 and TS-044742). The authors are indebted to Dr. Hedvig Medzihradszky-Schweiger for analyses and to Dr. György Túrós for recording the IR spectra.

References

[1] A. Togni, T. Hayashi (Eds.), Ferrocenes (Homogeneous Catalysis, Organic Synthesis, Materials Science), VCH Verlagsgessellschaft, Weinheim, 1995.

[2] (a) K.E. Dombrowki, W. Baldwin, J.E. Sheats, J. Organomet. Chem. 302 (1986) 281;
(b) P. Köpf-Maier, H. Köpf-Maier, Chem. Rev. 87 (1987) 1137;
(c) E.W. Neuse, M.G. Meirim, N.F. Blam, Organometallics 7 (1988) 2562;
(d) V. Scarcia, A. Furlani, B. Longato, B. Corain, G. Pilloni, Chim. Acta 67 (1988) 153;
(e) D.T. Hill, R.K. Johnson, P.D. Stupic, J.H. Zhang, W.M. Reiff, D.S. Egleston, Inorg. Chem. 28 (1989) 3529;
(f) E.W. Neuse, F. Kanzawa, Appl. Organomet. Chem. 4 (1) (1990) 19;
(g) N. Motohashi, R. Meyer, S.R. Gollapudi, R. Kesava, J. Organomet. Chem. 398 (1990) 205;
(h) A. Houlton, R.M.G. Roberts, J. Silver, J. Organomet. Chem. 418 (1991) 107;
(i) S. Top, J. Tang, A. Vessieres, D. Carrez, C. Prorot, G. Jaouen, Chem. Commun. (1996) 955;
(j) S. Top, A. Vessiéres, C. Cabestaing, I. Laios, G. Leclerq, C. Provot, G. Jaouen, J. Organomet. Chem. 637–639 (2001) 500;
(k) T. Klimova, E.I. Klimova, M. Martinez Garcia, E.A. Vázquez López, C. Alvarez Toledano, A.R. Toscano, L. Ruíz Ramírez, J. Organomet. Chem. 628 (2001) 107;
(l) H. Ma, Y. Hou, Y. Bai, J. Lu, B. Yang, J. Organomet. Chem. 637-639 (2001) 7427;
(m) L. Delhaes, H. Abessolo, C. Biot, L. Berry, P. Delcourt, L. Maciejewski, J. Brocard, D. Camus, D. Dive, Parasitol. Res. 87 (2001) 239;
(n) B. Weber, A. Serafin, J. Michie, C. Van Rensburg, J.C. Swarts, L. Bohm, Anticancer Res. 24 (2B) (2004) 763;
(o) G. Jaouen, S. Top, A. Vessieres, G. Leclercq, M.J. McGlinchey, Curr. Med. Chem. 11 (2004) 2505;
(p) C. Bincoletto, I.L.S. Tersariol, C.R. Oliviera, S. Dreher, D.M. Fausto, M.A. Soufen, A. Marco, F.D. Nascimento, A.C.F. Caires, Bioorg. Med. Chem. 13 (2005) 3047;
(q) E. Hillard, A. Vessieres, L. Thouin, G. Jaouen, C. Amatore, Angew. Chem., Int. Ed. 45 (2006) 285.

[3] (a) Á. Abrán, A. Csámpai, P. Sohár, Zs. Böcskei, Tetrahedron 55 (1999) 5441;
(b) Á. Abrán, A. Csámpai, A. Kotschy, O. Barabás, P. Sohár, J. Mol. Struct. 569 (2001) 185;
(c) V. Kudar, V. Zsoldos-Mády, K. Simon, A. Csámpai, P. Sohár, J. Organomet. Chem. 690 (2005) 4018;
(d) L. Găină, A. Csámpai, Gy. Túrós, T. Lovász, V. Zsoldos-Mády, I.A. Silberg, P. Sohár, Org. Biomol. Chem. 4 (2006) 4375;
(e) V. Zsoldos-Mády, A. Csámpai, R. Szabó, E. Mészáros-Alapi, J. Pásztor, F. Hudecz, P. Sohár, ChemMedChem 1 (2006) 1119.

[4] Gy.I. Túrós, A. Csámpai, M. Czugler, H. Wamhoff, P. Sohár, J. Organomet. Chem. 634 (2001) 122.

[5] Gy.I. Túrós, A. Csámpai, T. Lovász, A. Györfi, H. Wamhoff, P. Sohár, Eur. J. Org. Chem. (2002) 3801.
[6] A. Csámpai, Gy.I. Túrós, V. Kudar, K. Simon, H. Oeynhausen, H. Wamhoff, P. Sohár, Eur. J. Org. Chem. (2004) 717.
[7] A. Csámpai, Á. Abrán, V. Kudar, Gy.I. Túrós, H. Wamhoff, P. Sohár, J. Organomet. Chem. 690 (2005) 802.
[8] (a) O.S. Gardner, C.-W. Shiau, C.-S. Chen, L.M. Graves, J. Biol. Chem. 280 (2005) 10109;
(b) R.H. Mourao, T.G. Silva, A.L.M. Soares, E.S. Vieira, J.N. Santos, M.C.A. Lima, V.L.M. Lima, S.L. Galdino, J. Barbe, I.R. Pitta, Eur. J. Med. Chem. 40 (2005) 1129;
(c) G. He, Y.-M. Sung, J. DiGiovanni, S.M. Fischer, Cancer Res. 66 (2006) 1873;
(d) M. Metwally, H. Etman, E. Keshk, A. Fekry, Phosphorus, Sulfur Silicon Relat. Elem. 181 (2006) 1039;
(e) R.K. Hughes, E.J. Belfield, M. Muthusamay, A. Khan, A. Rowe, S.E. Harding, S.A. Fairhurst, S. Bornemann, R. Ashton, R.N.F. Thorneley, R. Casey, Biochem. J. 395 (2006) 641;
(f) J.-Q. Weng, D.-L. Shen, C.-X. Tan, X.-M. Ou, Youji Huaxue 26 (2006) 1106;
(g) D.-Y. Hu, B.-A. Song, W. He, S. Yang, L.-H. Jin, Hecheng Huaxue 14 (2006) 319.
[9] (a) K. Ohno, R. Tsutsumi, N. Matsumoto, H. Yamashita, Y. Amada, J.-I. Shishikura, H.I.S.I. Yatsugi, M. Okada, S. Sakamoto, T. Yamaguchi, J. Pharmacol. Exp. Ther. 306 (2003) 66;
(b) H. Yamashita, K. Ohno, Y. Amada, H. Hattori, Y. Ozawa-Funatsu, T. Toya, H. Inami, J.-I. Shishikura, S. Sakamoto, M. Okada, T. Yamaguchi, J. Pharmacol. Exp. Ther. 308 (2004) 127;
(c) H. Takuchi, T. Mizuno, G. Zhang, J. Wang, J. Kawanokuchi, R. Kuno, A. Suzumara, J. Biol. Chem. 280 (2005) 10444.
[10] (a) L. Servant, C. Cazaux, A. Bieth, S. Iwai, F. Hanaoka, J.S. Hoffmann, J. Biol. Chem. 277 (2002) 50046;
(b) L. Riou, E. Eveno, A. van Hoffen, A.A. van Zeeland, A. Sarasin, L.H.F. Mullenders, Cancer Res. 64 (2004) 889;
(c) R.L. Jarvest, S.A. Armstrong, J.M. Berge, P. Brown, J.S. Elder, M.J. Brown, R.C.B. Copley, A.K. Forrest, D.W. Hamprecht, P.J. O'Hanlon, D.J. Mitchell, S. Rittenhouse, D.R. Witty, Bioorg. Med. Chem. Lett. 14 (2004) 3937;
(d) Y. Takahashi, S.I. Moriwaki, Y. Sugiyama, Y. Endo, K. Yamazaki, T. Mori, M. Takigawa, S. Inoue, J. Invest. Dermatol. 124 (2005) 435;
(e) K.S. Atwal, S.V. O'Neil, S. Ahmad, L. Doweyko, M. Kirby, C.R. Dorso, G. Chandrasena, B-C. Chen, R. Zhao, R. Zahler, Bioorg. Med. Chem. Lett. 16 (2006) 4796;
(f) K. Sztanke, K. Pasternak, A. Sidor-Wojtowicz, J. Truchlinska, K. Jozwiak, Bioorg. Med. Chem. 14 (2006) 3635;
(g) K.-i. Shinohara, T. Bando, S. Sasaki, Y. Sakakibara, M. Minoshima, H. Sugiyama, Cancer Sci. 97 (2006) 219;
(h) A.V. Silamkoti, P.W. Allan, A.E.A. Hassan, A.T. Fowler, E.J. Sorscher, W.B. Parker, J.A. Secrist, Nucleos. Nucleot. Nucl. Acids 24 (2005) 881;
(i) Y. Ji, H.J. Lee, C. Goodman, M. Uskokovic, K. Liby, M. Sporn, N. Suh, Mol. Cancer Ther. 5 (2006) 1452.
[11] (a) D.R. Hannah, E.C. Sherer, R.V. Davies, R.B. Titman, C. Laughton, M.F. Stevens, Bioorg. Med. Chem. 8 (2000) 739;
(b) J. Wu, Y.-P. Sun, P.-Z. Zhang, Q.-S. Yu, Youji Huaxue 24 (2004) 1403;
(c) J. Li, Y.F. Zhao, X.L. Zhao, X.Y. Yuan, P. Gong, Arch. Pharm. 339 (2006) 593;
(d) S. Palwinder, P. Kamaldeep, Bioorg. Med. Chem. 14 (2006) 8622;
(e) C. Carnrot, S.R. Vogel, Y. Byun, L. Wang, W. Tjarks, S. Eriksson, A.J. Phipps, Biol. Chem. 387 (2006) 1575;
(f) B.R. Hearn, D. Zhang, Y. Li, D.C. Myles, Biol. Chem. 387 (2006) 1575;
(g) T. Emura, N. Suzuki, A. Fujioka, H. Ohshimo, M. Fukushima, Int. J. Oncol. 27 (2005) 449;
(h) F. Xie, S. Li, D. Bai, L. Lou, Y. Hu, J. Comb. Chem. 9 (2007) 12.
[12] J. Boichard, J.P. Monin, J. Tirouflet, Bull. Soc. Chim. Fr. 4 (1963) 851.
[13] P. Nagy, A. Csámpai, D. Szabó, J. Varga, V. Harmat, F. Ruff, Á. Kucsman, J. Chem. Soc., Perkin Trans. 1 (2001) 339.
[14] S. Miertus, E. Scrocco, J. Tomasi, J. Chem. Phys. 55 (1981) 117.
[15] (a) J.B. Hendrickson, R. Rees, J.F. Templeton, J. Am. Chem. Soc. 86 (1964) 107;
(b) A. Ramazani, S.A. Hossaini-Alemi, Phosphorus, Sulfur Silicon Relat. Elem. 176 (2001) 237;
(c) A. Ramazani, A.R. Kazemizadeh, B. Ganjeie, E. Ahmadi, Asian J. Chem. 17 (2005) 2375;
(d) N.A. Danilkina, L.E. Mikhailov, B.A. Ivin, Russ. J. Org. Chem. 42 (2006) 783.
[16] (a) J.W. Lown, J.C.N. Ma, Can. J. Chem. 45 (1967) 938;
(b) E. Winterfeldt, J.M. Nelka, Chem. Ber. 100 (1967) 3671;
(c) L.I. Giannola, S. Palazzo, P. Agozzino, L. Lamartina, L. Ceraulo, J. Chem. Soc., Perkin Trans. 1 11 (1978) 1428;
(d) P. Sohár, Zs. Szőke-Molnár, G. Stájer, G. Bernáth, Magn. Res. Chem. 27 (1989) 959.
[17] (a) P. SohárNuclear Magnetic Resonance Spectroscopy, vol. 2, CRC Press, Boca Raton, FL, 1983, pp. 153–154;
(b) P. SohárNuclear Magnetic Resonance Spectroscopy, vol. 2, CRC Press, Boca Raton, FL, 1983, p. 185;
(c) P. SohárNuclear Magnetic Resonance Spectroscopy, vol. 2, CRC Press, Boca Raton, FL, 1983, p. 89;
(d) P. SohárNuclear Magnetic Resonance Spectroscopy, vol. 3, CRC Press, Boca Raton, FL, 1983, pp. 4–6;
(e) P. SohárNuclear Magnetic Resonance Spectroscopy, vol. 2, CRC Press, Boca Raton, FL, 1983, p. 61;
(f) P. SohárNuclear Magnetic Resonance Spectroscopy, vol. 1, CRC Press, Boca Raton, FL, 1983, pp. 194–196.
[18] S. Holly, P. Sohár, in: L. Láng, W.H. Prichard (Eds.), Theoretical and Technical Introduction to the Series "Absorption Spectra in the Infrared Region", vol. 87, Akadémiai Kiadó, Budapest, 1975.
[19] K. Wolinski, J.F. Hilton, P. Pulay, J. Am. Chem. Soc. 112 (1990) 8251.
[20] K. Raghavachari, G.W. Trucks, J. Chem. Phys. 91 (1989) 1062.
[21] M.J. Frisch et al., Gaussian: GAUSSIAN 98 (Revision A.1), Gaussian Inc., Pittsburgh, PA, 1998.
[22] J.H. Noggle, R.E. Schirmer, The Nuclear Overhauser Effect, Academic Press, New York, 1971.
[23] J.K.M. Sanders, J.D. Mersch, Prog. Nucl. Magn. Reson. 15 (1982) 353–400.
[24] D.T. Pegg, D.M. Doddrell, M.R. Bendall, J. Chem. Phys. 77 (1982) 2745.
[25] M.R. Bendall, D.M. Doddrell, D.T. Pegg, W.E. Hull, High Resolution Multipulse NMR Spectrum Editing and DEPT, Bruker, Karlsruhe, 1982.
[26] (a) R.R. Ernst, G. Bodenhausen, A. Wokaun, Principles of Nuclear Magnetic Resonance in one and Two Dimensions, Clarendon Press, Oxford, UK, 1987, pp. 400–448;
(b) R.R. Ernst, G. Bodenhausen, A. Wokaun, Principles of Nuclear Magnetic Resonance in one and Two Dimensions, Clarendon Press, Oxford, UK, 1987, pp. 471–479.
[27] (a) J.K.M. Sanders, B.K. Hunter, Modern NMR Spectroscopy. A Guide for Chemists, University Press, Oxford, UK, 1987, pp. 108–113;
(b) J.K.M. Sanders, B.K. Hunter, Modern NMR Spectroscopy, A Guide for Chemists, University Press, Oxford, UK, 1987, pp. 94–97, 100–107.
[28] A. Bax, G. Morris, J. Magn. Res. 42 (1981) 501–505.
[29] H. Kessler, C. Griesinger, J. Zarboch, H. Loosli, J. Magn. Res. 57 (1984) 331–336.
[30] G.M. Sheldrick, SHELXS97—Program for Crystal Structure Determination, University of Göttingen, Germany, 1997.

[31] G.M. Sheldrick, SHELXL97—Program for the Refinement of Crystal Structures, University of Göttingen, Germany, 1997.
[32] A.C.T. North, D.C. Phillips, F.S. Mathews, Acta Crystallogr., A 24 (1968) 351–359.
[33] PATTY: P.T. Beurskens, G. Admiraal, G. Beurskens, W.P. Bosman, S. Garcia-Granda, R.O. Gould, J.M.M. Smits, C. Smykalla. The DIRDIF program system, Technical Report of the Crystallography Laboratory, University of Nijmegen, The Netherlands, 1992.
[34] SIR92: A. Altomare, M. Cascarano, C. Giacovazzo, A. Guagliardi, J. Appl. Cryst. 26 (1994) 343.
[35] teXsan for Windows version 1.06: Crystal Structure Analysis Package, Molecular Structure Corporation, 1997–1999.